

Aizhuo Liu  
Roland Riek  
Ralph Zahn  
Simone Hornemann  
Rudi Glockshuber  
Kurt Wüthrich  
Institut für Molekularbiologie  
und Biophysik,  
Eidgenössische Technische  
Hochschule,  
CH-8093 Zürich, Switzerland

---

## Peptides and Proteins in Neurodegenerative Disease: Helix Propensity of a Polypeptide Containing Helix 1 of the Mouse Prion Protein Studied by NMR and CD Spectroscopy

**Abstract:** Transmissible spongiform encephalopathies (TSE) or “prion diseases” have been related to the “protein-only hypothesis”, which suggests that the “scrapie form (PrP<sup>Sc</sup>)” of the prion protein (PrP) is the TSE infectious agent. The nmr structure of the ubiquitous benign cellular form of PrP (PrP<sup>C</sup>) consists of a globular domain of residues 126–231 with three  $\alpha$ -helices and a short  $\beta$ -sheet, and a flexible extended “tail” of residues 23–125. The peptide segment of helix 1 has been implicated in various stages of hypothetical pathways to prion pathology on the basis of the protein-only idea, including that it takes part in the conformation change that leads from PrP<sup>C</sup> to PrP<sup>Sc</sup>. In this paper we describe solution nmr and circular dichroism studies of the synthetic hexadecapeptide mPrP(143–158), with the sequence H-NDWEDRYRENMYRYP-NH<sub>2</sub>, where the bold letters represent the segment that forms helix 1 in murine PrP<sup>C</sup>. In both H<sub>2</sub>O and a 1:1 mixture of H<sub>2</sub>O and trifluoroethanol this polypeptide segment shows high helix propensity, which is a key issue in discussions on potential roles of this molecular region in conformational transitions of PrP. © 1999 John Wiley & Sons, Inc. Biopoly 51: 145–152, 1999

**Keywords:** transmissible spongiform encephalopathies; protein-only hypothesis; polypeptides in neurodegenerative disease; nmr structure determination; helix propensity of a prion protein fragment

---

### PREAMBLE

For the opening lecture of the 6th Naples Workshop on Bioactive Peptides, K.W. proposed the title “Conformational Polymorphism of Peptides and Proteins in Neurodegenerative Diseases” and submitted the following abstract: “Prions are a novel class of infectious pathogens that are distinct from bacteria, viruses or

viroids, and in which nucleic acids are apparently not essential for the propagation of the infectious agent. Prion diseases, or transmissible spongiform encephalopathies (TSE), include scrapie in sheep, bovine spongiform encephalopathy (BSE), and kuru, Creutzfeldt–Jakob disease (CJD), fatal familial insomnia (FFI) and the Gerstmann–Sträussler–Scheinker syndrome (GSS) in humans. The protein-only

---

Correspondence to: K. Wüthrich. Phone: +41 1 633 2473. Fax: +41 1 633 1151

Contract grant sponsor: Schweizerischer Nationalfonds  
Contract grant numbers: 438+.50287 and 438+.50285

Biopolymers (Peptide Science), Vol. 51, 145–152 (1999)

© 1999 John Wiley & Sons, Inc.

CCC 0006-3525/99/020145-08

hypothesis suggests that onset of TSEs is related to a conformational transition of the ubiquitous cellular form of the prion protein in mammalian tissues, PrP<sup>C</sup>, into an aggregated infectious form, PrP<sup>Sc</sup>. It is a unique challenge for protein science that a group of lethal diseases should thus be linked entirely with a change of conformation of a natural polypeptide chain. Nmr structural studies have been performed with recombinant fragments of various lengths from the human, bovine, and murine PrPs, including the intact proteins comprising residues 23–231. The results obtained so far bear on the PrP<sup>C</sup> form of the prion protein. The globular structure of the C-terminal domain 126–231, as determined in the polypeptide fragment *mPrP*(121–231),<sup>1</sup> was found to be preserved in the intact protein, and the N-terminal polypeptide segment 23–125 is flexibly disordered.<sup>2</sup> This structural information has been obtained from experiments with uniformly <sup>15</sup>N-labeled and <sup>15</sup>N, <sup>13</sup>C-doubly-labeled proteins. The linewidths in heteronuclear <sup>1</sup>H–<sup>15</sup>N correlation spectra and the <sup>15</sup>N{<sup>1</sup>H}-NOEs showed that the well-structured residues 126–230 have correlation times of several nanoseconds, as is typical for small globular proteins, whereas correlation times shorter than 1 nanosecond were observed for all residues outside of this domain. Implications of this structural data for various aspects of the transition of PrP<sup>C</sup> to PrP<sup>Sc</sup> will be discussed. Recently it was discovered that a novel nmr approach, TROSY (transverse relaxation-optimized spectroscopy), enables solution nmr studies with very large molecular sizes.<sup>3</sup> This technique should, in principle, also enable studies of aggregated forms of the prion protein.” The lecture then focused on the implications of the nmr structure of PrP<sup>C</sup> for the transformation into PrP<sup>Sc</sup> and on the potentialities of TROSY for investigations of very large homo-oligomeric proteins, possibly including aggregated states of the prion protein. In this written version of the presentation we adhere more faithfully to the workshop theme “Bioactive Peptides” and describe new, so far unpublished data obtained with CD and nmr investigations of the polypeptide fragment *mPrP*(143–158) from the amino acid sequence of murine PrP.

## INTRODUCTION

The helix 1 in the nmr structure of the recombinant murine prion protein (*mPrP*)<sup>1,2</sup> contains 11 amino acid residues, of which 6 are either positively or negatively charged at neutral pH. In the three-dimensional structure of *mPrP*<sup>C</sup> this helix is set apart from the protein core,<sup>1</sup> and in secondary structure predictions it has not

been recognized as a helix.<sup>4–6</sup> The N-terminal half of helix 1 is part of the epitope of the PrP<sup>Sc</sup>-specific monoclonal antibody 15B3 and is the epitope of the antibody 6H4, which recognizes recombinant PrP as well as PrP<sup>C</sup>.<sup>7</sup> It has also been suggested that helix 1 might be part of the peptide sequence that is involved in the conformation change leading from PrP<sup>C</sup> to PrP<sup>Sc</sup>.<sup>8</sup> To further investigate the  $\alpha$ -helix propensity of the amino acid sequence of helix 1 we investigated the solution conformation of the synthetic polypeptide *mPrP*(143–158), H-NDWEDRYRENMYRYP-NH<sub>2</sub>, where the segment corresponding to helix 1 of *mPrP*<sup>C</sup> is indicated in bold. These measurements were performed at pH 4.5 and 20°C, i.e., under the same conditions that had been used for the determination of the solution structures of *mPrP*(121–231) and *mPrP*(23–231). As is commonly observed for short linear polypeptides in solution,<sup>9–11</sup> one would anticipate to have mixtures of structured and unfolded forms in solutions of this peptide, which are in rapid exchange on the chemical shift time scale unless the rearrangement involves peptide *cis*–*trans* isomerization.<sup>9</sup> For the conformational analysis we therefore adopted the strategy of estimating the population of structured forms from the amide proton– $\alpha$ -proton coupling constants <sup>3</sup>*J*<sub>HN $\alpha$</sub> , from the <sup>13</sup>C $\alpha$  chemical shifts, and from circular dichroism (CD) spectroscopy. In addition to the aqueous solution, the peptide was studied in mixed solvents obtained by addition of variable amounts of trifluoroethanol (TFE). The structure of a predominant folded form was then derived from medium-range and long-range nuclear Overhauser effects (NOE),<sup>12</sup> using the assumption that the contributions to these NOEs from all other populated conformations are negligibly small.

## EXPERIMENTAL PROCEDURES

The peptide *mPrP*(143–158), with the amino acid sequence H-NDWEDRYRENMYRYP-NH<sub>2</sub>, was synthesized for us by Dr. Jens Schneider (Jerini Biotools, Berlin) using the standard solid-phase method. It was purified to homogeneity by reversed-phase C<sub>18</sub> HPLC, using water and acetonitrile with 0.1% trifluoroacetic acid as the solvent system. A gradient from 0 to 20% acetonitrile in 30 min gave efficient separation, as detected at 215 nm. The peptide structure and homogeneity were confirmed by analytical HPLC and by mass spectrometry.

## NMR Spectroscopy

Nmr samples were prepared by dissolving the lyophilized peptide at about 1 mM concentration in 550  $\mu$ L of either 90% H<sub>2</sub>O/10% D<sub>2</sub>O or mixed solvents containing 10–50%

(v/v) TFE- $d_4$  in  $H_2O$ . The pH was adjusted to 4.5 by addition of small amounts of NaOH or HCl. Nmr spectra were collected on a Bruker DRX 500 spectrometer at 20°C. To obtain sequence-specific resonance assignments, 2QF-COSY spectra,<sup>13</sup> clean-TOCSY spectra<sup>14</sup> with a mixing time of 70 ms, and NOESY<sup>15</sup> and ROESY<sup>16</sup> spectra with mixing times of 100–350 ms were recorded. Chemical shifts were referenced to DSS, with  $H_2O$  at 4.80 ppm at 20°C, and using the common coefficients for referencing of the  $^{13}C$  chemical shifts.

In the data handling the residual water signal after preirradiation was further reduced using the convolution method of Marion et al.<sup>17</sup> Prior to Fourier transformation the time domain data were multiplied with a sine bell window shifted by  $\pi/2$ .<sup>18</sup> Baseline distortions were corrected using the FLATT procedure.<sup>19</sup> Processing of the spectra was performed with the program PROSA.<sup>20</sup> Peak picking in the nmr spectra, spin system identification and volume integration of the NOESY cross peaks were carried out with the interactive program XEASY.<sup>21</sup> Values of the  $^3J_{HN\alpha}$  scalar coupling constants were obtained by inverse Fourier transformation and time-domain fitting of cross sections taken through in-phase NOESY cross peaks,<sup>22</sup> so that this information was derived from the same data sets as the NOE distance constraints. The  $^3J_{\alpha\beta}$  coupling constants for residues with  $C^\beta H_2$  groups were determined from E.COSY spectra.<sup>23</sup>

### Circular Dichroism Spectroscopy (CD)

CD spectra were collected at 20°C on a Jasco model 710 spectropolarimeter interfaced with a Neslab RTE-110 water bath. Measurements were carried out in a 0.5 mm path length quartz cuvette, and the results are expressed as the mean residue ellipticity at 222 nm,  $\Theta_{222}$ . During thermal denaturation experiments the temperature was increased at a linear rate of 50 deg/h.

### Structure Calculation and Analysis

Structure calculations were performed with the torsion angle dynamics program DYANA,<sup>24</sup> using an input consisting exclusively of medium-range and long-range NOE upper distance constraints. The DYANA conformers with the lowest residual target function values were energy-minimized in a 6 Å thick shell of water molecules using the AMBER all-atom force field<sup>25</sup> as implemented in the program OPAL.<sup>26</sup> The program MOLMOL<sup>27</sup> was used for the analysis and presentation of the results of the structure determination.

## RESULTS AND DISCUSSION

The sequential assignment approach based on homonuclear 2D  $^1H$  nmr<sup>12</sup> was used to obtain complete sequence-specific  $^1H$  nmr assignments. Sequential

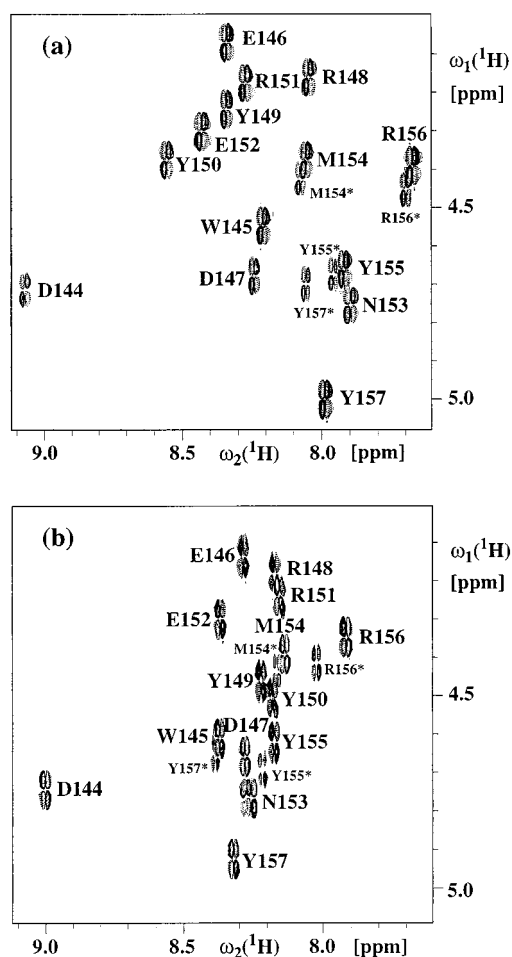


**FIGURE 1** Fingerprint region of 2D [ $^1H$ ,  $^1H$ ]-COSY spectra of the peptide *mPrP*(143–158): (a) solvent TFE/water 1:1 (v/v); (b) solvent water. The data were recorded at 20°C and pH 4.5. Assignments of cross peaks are denoted with the one-letter code for the amino acids and the sequence numbers. For each of the residues 154–157 two peaks were identified, and the less abundant species is identified by smaller lettering and an asterisk.

connectivities for two complete sets of spin systems were found for the C-terminal pentapeptide segment from Met 154 to Pro 158. In the major form, the strong  $d_{\alpha\delta}$  sequential connectivities between Tyr 157 and Pro 158 showed that the Tyr 157–Pro 158 peptide bond is in the *trans* conformation.<sup>12</sup> For the second form, a strong  $d_{\alpha\alpha}$  cross peak showed that the Tyr 157–Pro 158 peptide bond is in the *cis* form. Measurement of the resonance intensities corresponding to the two species (Fig. 1) gives an abundance ratio of about 1:5 for this *cis* : *trans* equilibrium at the C-terminal Pro 158.<sup>9</sup> Chemical shift tables for the peptide *mPrP*(143–158) at TFE concentrations of 0%, 10%, 25%, and 50% have been deposited with the Bio Mag Res Bank (e-mail: elu@nmrfam.wisc.edu).

## Estimates of the Helix-Coil Conformational Equilibrium from $\alpha$ -Carbon Chemical Shifts and Amide Proton- $\alpha$ -Proton Coupling Constants

On the basis of the assumption that the solutions of *mPrP*(143–158) contain the  $\alpha$ -helical conformation in equilibrium with a manifold of unfolded coils, which all have random coil  $^{13}\text{C}^\alpha$  chemical shifts and  $^3J_{\text{HN}\alpha}$  scalar coupling constants, we used these two nmr parameters to assess the population of the helical form. Figure 2 shows plots of  $\Delta\delta(^{13}\text{C}^\alpha)$ , the difference between the measured values of  $^{13}\text{C}^\alpha$  chemical shifts and the corresponding “random coil” shifts, versus the sequence of *mPrP*(143–158). The data show for all water/TFE mixtures that the octapeptide segment 143–151 has high helix content, significantly less helix character is evidenced for the residues 152–154, and the residues 143 and 155–158 show no evidence for helical structure. Using the corresponding shifts in the nmr solution structure of *mPrP*(121–231)<sup>28</sup> to represent 100% helix population, the helix populations listed in the first column of Table I were derived for the segment 144–151, which yielded values up to 82% in 50% TFE. In the framework of a rapid equilibrium, on the chemical shift time scale, between a helix and an ensemble of random coils, and assuming that typical values of  $^3J_{\text{HN}\alpha}$  are 3.9 Hz for an  $\alpha$ -helix and 7.0 Hz for a “random coil”, the  $^3J_{\text{HN}\alpha}$  values (Fig. 3) have been used to obtain a second, independent estimate of the  $\alpha$ -helix population.<sup>29</sup> The coupling

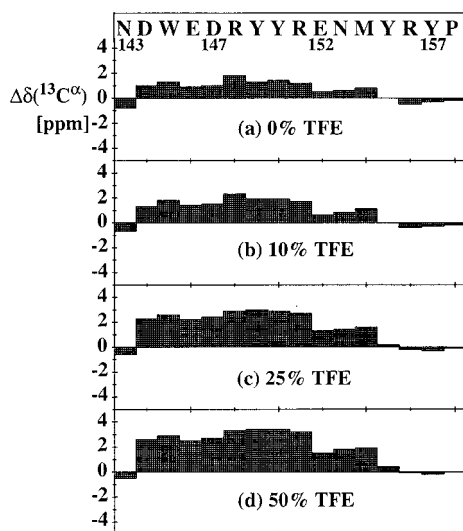


**FIGURE 2** Conformation-dependent  $^{13}\text{C}^\alpha$  chemical shifts,  $\Delta\delta(^{13}\text{C}^\alpha)$ , of the peptide *mPrP*(143–158) (sequence at the top) in TFE/water mixtures with variable TFE content (v/v) at 20°C and pH 4.5. Positive (downfield)  $^{13}\text{C}^\alpha$  chemical shifts are indicative of helical conformation.<sup>38</sup>

**Table I** Population of  $\alpha$ -Helical Structure in the Octapeptide Segment 144–151 in the Peptide *mPrP*(143–158) in Different TFE/ $\text{H}_2\text{O}$  Mixtures

| Helix Population for Residues 144–151 (%) |  |                           |
|---|--|---------------------------|
| % TFE (v/v)                               | $\Delta\delta(^{13}\text{C}^\alpha)^a$ | $^3J_{\text{HN}\alpha}^b$ |
| 50  | 82                                     | 87                        |
| 25  | 72                                     | 83                        |
| 10  | 47                                     | 66                        |
| 0   | 34                                     | 42                        |

<sup>a</sup> Estimated by comparison of the conformation-dependent  $^{13}\text{C}^\alpha$  chemical shifts of *mPrP*(143–158),  $\Delta\delta(^{13}\text{C}^\alpha)$ , with those of the corresponding peptide sequence in the nmr structure of *mPrP*(121–231).<sup>28</sup>

<sup>b</sup> Estimated by the method of Bradley et al.,<sup>29</sup> using 3.9 Hz and 7.0 Hz as the  $\alpha$ -helix and random coil coupling constants, respectively.

data confirm the high propensity for helix formation in the segment 143–151 and give slightly higher helix propensity for these residues than the  $^{13}\text{C}^\alpha$  shifts (Table I).

## CD Studies of the Helix-Coil Conformational Equilibrium

In aqueous solutions of *mPrP*(143–158) at pH 4.5 and 7.0 there was no concentration effect on the molar ellipticity in the range of 10–500  $\mu\text{M}$ . These solutions were titrated with TFE from 0 to 80% (v/v) (Fig. 4a). The  $\alpha$ -helix population increased gradually with the addition of TFE, as judged from the characteristic negative CD bands at 208 nm and 222 nm and a positive band at 193 nm. The two recordings of  $\Theta_{222}$  versus the TFE concentration at the two different pH values are very similar, indicating that the conformation is not significantly affected by pH in the range from 4.5 to 7.0. The helix population for residues 144–151 estimated from the CD data corresponds quite well with the results derived using nmr (Table I). The thermal denaturation of the peptide followed by  $\Theta_{222}$  shows a very broad transition (Fig. 4b), indicating that unfolding and refolding occur with very low cooperativity, as expected for a small peptide without long-range interactions.<sup>30,31</sup> The thermal stability is significantly higher in 1:1  $\text{H}_2\text{O}$ /TFE than in  $\text{H}_2\text{O}$ .

## Conformation of the Helical Form of *mPrP*(143–158)

As is commonly observed for short linear peptides, the conformational equilibria in aqueous solution of

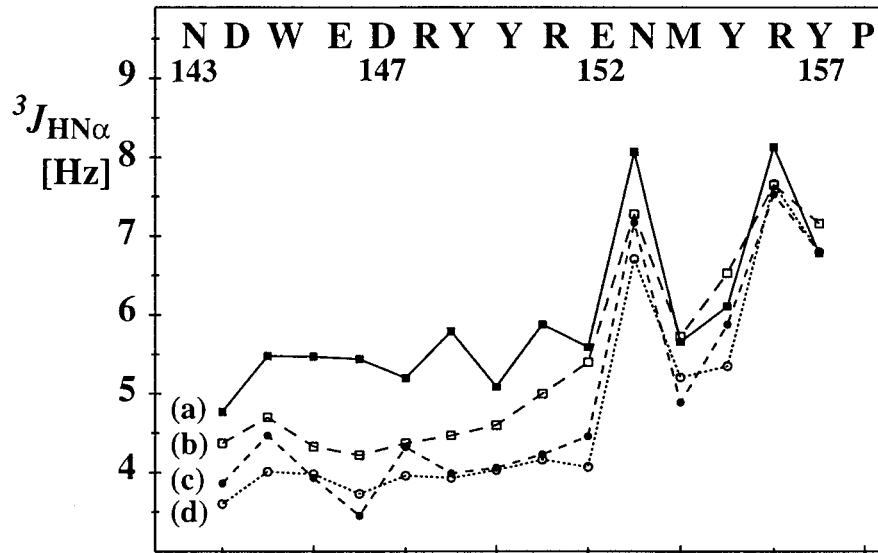


**FIGURE 3**  $^3J_{\text{HN}\alpha}$  coupling constants of the peptide *mPrP*(143–158) measured in TFE/water mixtures with the following TFE contents (v/v): (a) 0%; (b) 10%; (c) 25%; (d) 50%. The data were measured at 20°C and pH 4.5. Segments of several successive residues with  $^3J_{\text{HN}\alpha}$  coupling constants smaller than 6 Hz are indicative of helical conformation.<sup>12</sup>

*mPrP*(143–158) are shifted toward the helical form by the addition of TFE (Figs. 2–4).<sup>32,33</sup> We therefore used the data collected in a 1:1 mixture of water and TFE as input for a structure determination of the helical species. Two observations made in Figures 2–4 and in Table I provide support for this approach: (i) In pure water the helix population is about 30–40%, showing that the addition of TFE enhances intrinsic helix propensity. (ii) Both the  $^{13}\text{C}\alpha$  shifts (Fig. 2) and  $^3J_{\text{HN}\alpha}$  couplings (Fig. 3) indicate that helix formation involves the segment of residues 144–151 in *mPrP*(143–158). Helical structure in this segment is implicated also by the  $d_{\text{NN}}$  sequential NOEs and the medium-range NOEs (Fig. 5). As far as the backbone conformation is concerned, we thus have consistent data in the solutions with different TFE contents, with helical structure implicated for nearly three turns, from residues 144 to 151.

Several side chain–side chain NOEs between  $\delta\text{NH}_2$  of Asn 143 and the  $\gamma\text{CH}_2$  protons of Glu 146 and between  $\beta\text{CH}_2$  of Asn 143 and  $\beta\text{CH}_2$  and  $\gamma\text{CH}_2$  of Glu 146 have been observed (Fig. 6), which suggests the presence of side chain–side chain hydrogen bonding between the  $\delta$  protons of Asn 143 and the  $\varepsilon$  oxygen atoms of Glu 146. This qualitative interpretation of the NOE data is in agreement with the result of a structure calculation (Fig. 7a,b). The side chains of the two residues 143 and 146 are involved in mutual interactions that may suppress end fraying and thus stabilize the helix. The same local structure element has been observed at the start of helix 1 in the nmr

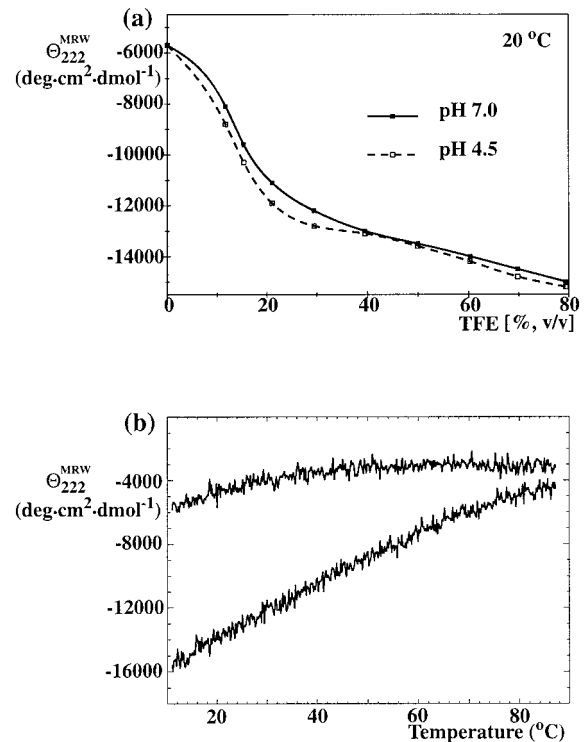


**FIGURE 4** (a) Mean residue molar ellipticity,  $\Theta_{222}^{\text{MRW}}$ , from CD spectra of the peptide *mPrP*(143–158) at 222 nm measured in mixed solvents of  $\text{H}_2\text{O}$  and TFE with variable TFE content (in % v/v),  $T = 20^\circ\text{C}$ , two different pH values as indicated. (b) Thermal denaturation curves of the peptide *mPrP*(143–158) at pH 4.5 in water and 50% (v/v) TFE/water, respectively. Both curves were measured with a linear temperature gradient of 50 deg/h.

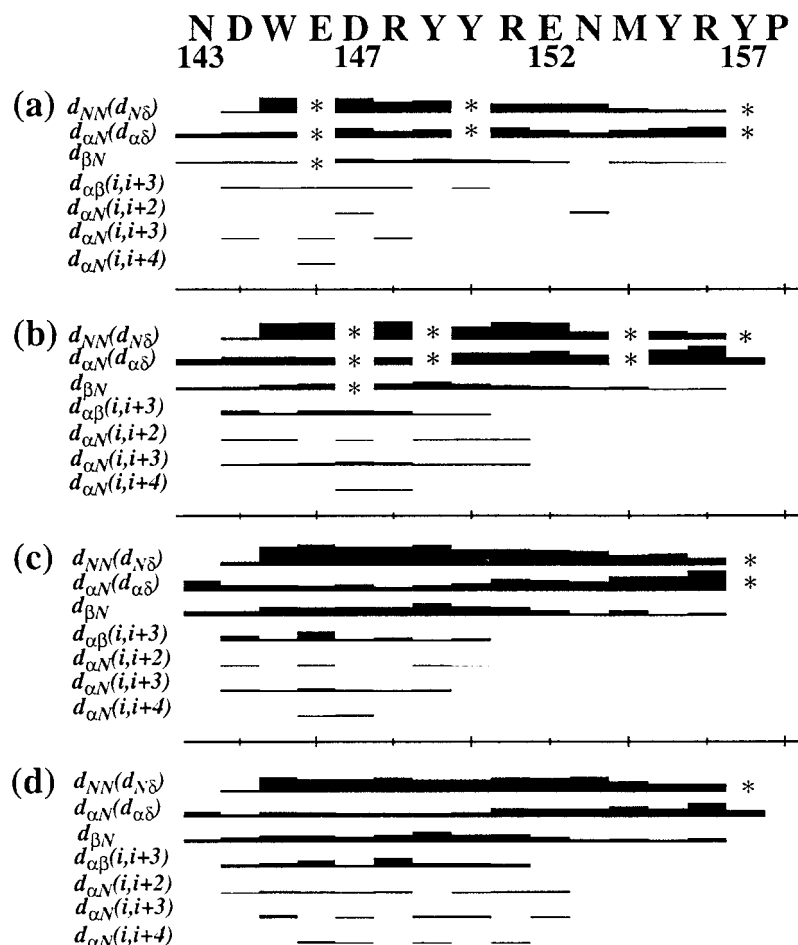


**FIGURE 5** Sequential and medium-range NOE connectivities in the peptide *mPrP*(143–158) (sequence at the top) in different TFE/water mixtures at 20°C and pH 4.5: (a) 0% TFE; (b) 10% TFE; (c) 25% TFE; (d) 50% TFE. The thickness of the lines reflects the relative intensities of the NOEs within the individual plots (a) to (d).  $d_{NN}$ ,  $d_{\alpha N}$ , and  $d_{\beta N}$  ( $d_{N\delta}$  and  $d_{\alpha\delta}$  for Xxx-Pro dipeptides) represent sequential NOE connectivities;  $d_{\alpha\beta}(i, i + 3)$ ,  $d_{\alpha N}(i, i + 2)$ ,  $d_{\alpha N}(i, i + 3)$  and  $d_{\alpha N}(i, i + 4)$  are medium-range NOE connectivities between  $\alpha$ - and  $\beta$ -protons or between  $\alpha$ - and amide protons.<sup>12</sup> An asterisk (\*) indicates that the sequential NOE could not be observed due to overlap either with other lines of the peptide or with the solvent signal.

structure of *mPrP*(121–231)<sup>34</sup> (Fig. 7c). This “pincette motif” appears to have a similar impact as the more common N-caps.<sup>35–37</sup> It is then of interest that no main chain–side chain NOEs between the backbone amide proton of Asn 143 and  $\beta\text{CH}_2$  of Glu 146 are observed at the start of helix 1 in *mPrP*, which has the sequence NDWED, since Asn has, according to statistics, a high preference to be an N-cap residue and Glu has a high propensity to be at the  $i + 3$  position.<sup>35</sup> The overall N-cap propensity is probably decreased by the low propensity of the Asp and Trp residues for the N-cap positions  $i + 1$  and  $i + 2$ , respectively.<sup>37</sup> In particular, the large hydrophobic Trp 145 side chain might sterically interfere with hydrogen bond formation between the backbone

amide proton of Asn 143 and the  $\epsilon$  oxygen atom of Glu 146, which could contribute to the apparent preference for the aforementioned “pincette” motif.

The helix 1 in *mPrP*(121–231) extends from residues 144 to 154. For *mPrP*(143–158) this helix length is also seen in Figure 2, but the helix population for the residues 152–154 is rather low. The conformational polymorphism observed for residues 154–158 in *mPrP*(143–158) (Fig. 1), which is related to *cis-trans* isomerization of the C-terminal proline, indicates that this polypeptide segment in *mPrP*(143–158) has no or only weak propensity for a preferred secondary structure and that its conformation is therefore dominated by the Tyr 157–Pro 158 peptide bond *cis-trans* equilibrium.<sup>9</sup>

In conclusion, the present study establishes that the polypeptide segment of helix 1 in *mPrP* has significant intrinsic helical propensity. The helix formed by the peptide *mPrP*(143–158) is similar to helix 1 in *mPrP*(121–231), including that an N-terminal “pin-cette motif” is found in both structures (Fig. 7). The polypeptide segment of helix 1 thus seems to be an initiation site for helix formation, and it is maintained as a helix in the intact protein. On this basis it would be no surprise if the globular domains of *mPrP* and, in particular, helix 1 were preserved during the conformational transition from  $\text{PrP}^{\text{C}}$  to  $\text{PrP}^{\text{Sc}}$ , as has been hypothesized in view of structural data collected with intact *mPrP*(23–231).<sup>2</sup>

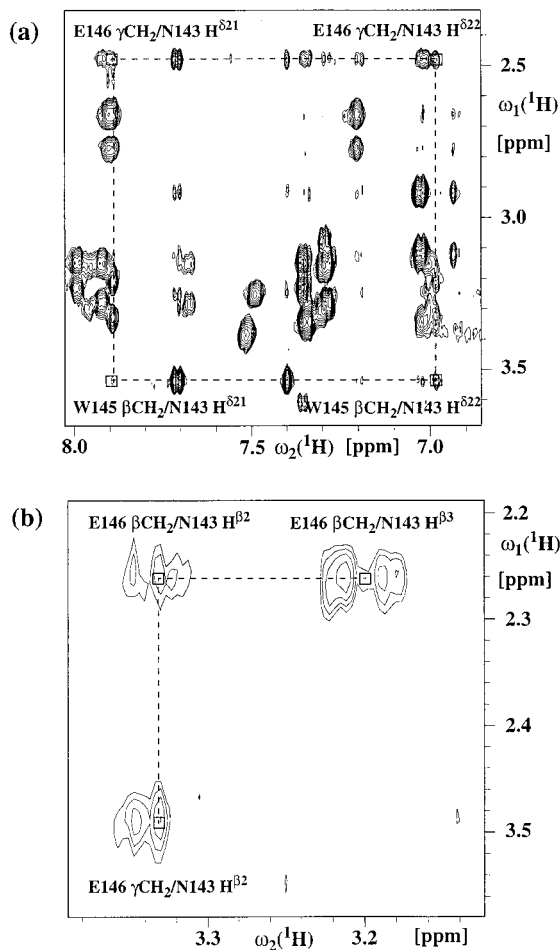


**FIGURE 6** 2D [ $^1\text{H}$ ,  $^1\text{H}$ ]-NOESY spectrum of *mPrP*(143–158) at 20°C and pH 4.5 recorded with a mixing time of 200 ms. (a) Region containing amide proton–aliphatic proton cross peaks. (b) Region containing cross peaks between different aliphatic protons. The dashed lines connect cross peaks involving side chain protons of the residues Asn 143, Trp 145, and Glu 146. The individual connectivities are boxed and identified with the one-letter amino acid code, the sequence number, and the type of hydrogen atom.

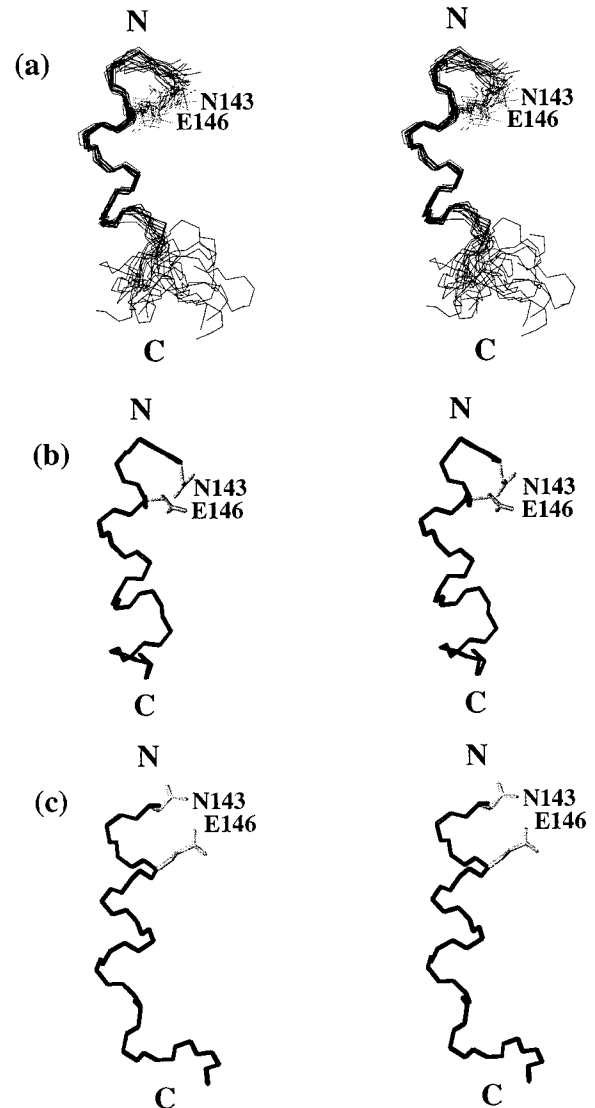


**FIGURE 7** (a,b) Stereoviews of the nmr structure of the peptide *mPrP*(143–158) in a mixed solvent of  $\text{H}_2\text{O}/\text{TFE}$  (v/v) = 1:1: (a) superposition of 20 energy-minimized DYANA conformers for best fit of backbone atoms from Asn 143 to Met 154; (b) conformer with the smallest RMSD to the mean structure; (c) nmr mean structure of helix 1 from residues 144–154 in *mPrP*(121–231).<sup>37</sup> The backbone (black lines) and the side chains of residues Asn 143 and Glu 146 (gray lines) are shown. At the N-terminus the side chains of Asn 143 and Glu 146 form a “pincette” motif (see text) both in the presently studied hexadecapeptide and in *mPrP*(121–231).

Financial support was obtained from the Schweizerischer Nationalfonds (Projects 438+.50287 (K.W.) and 438+.50285 (R.G.)) and an exchange fellowship of the ETH Zürich to A.L. We are grateful to D. Braun and R. Brunisholz for help with the CD measurements and the purification of the peptides, respectively.

## REFERENCES

1. Riek, R.; Hornemann, S.; Wider, G.; Billeter, M.; Glockshuber, R.; Wüthrich, K. *Nature* 1996, 382, 180–182.
2. Riek, R.; Hornemann, S.; Wider, G.; Glockshuber, R.; Wüthrich, K. *FEBS Lett* 1997, 413, 282–288.
3. Pervushin, K.; Riek, R.; Wider, G.; Wüthrich, K. *Proc Natl Acad Sci USA* 1997, 94, 12366–12371.
4. Huang, Z.; Gabriel, J.-M.; Baldwin, M. A.; Fletterick, R. J.; Prusiner, S. B.; Cohen, F. E. *Proc Natl Acad Sci USA* 1994, 91, 7139–7143.
5. Zhang, H.; Kaneko, K.; Nguyen, J. T.; Livshits, T. L.; Baldwin, M. A.; Cohen, F. E.; James, T. L.; Prusiner, S. B. *J Mol Biol* 1995, 250, 514–526.
6. Huang, Z.; Prusiner, S. B.; Cohen, F. E. *Folding Des* 1996, 1, 13–19.
7. Korth, C.; Stierli, B.; Streit, P.; Moser, M.; Schaller, O.; Fischer, R.; Schulz-Schaeffer, W.; Kretschmar, H.; Raeber, A.; Braun, U.; Ehrensperger, F.; Hornemann, S.; Glockshuber, R.; Riek, R.; Billeter, M.; Wüthrich, K.; Oesch, B. *Nature* 1997, 390, 74–77.
8. Prusiner, S. B. *Proc Natl Acad Sci USA* 1998, 95, 13363–13383.
9. Grathwohl, Ch.; Wüthrich, K. *Biopolymers* 1976, 15, 2025–2041.
10. Bundi, A.; Wüthrich, K. *Biopolymers* 1979, 18, 299–311.
11. Dyson, H. J.; Wright, P. E. *Nat Struct Biol* 1998, 5, 499–503.
12. Wüthrich, K. *NMR of Proteins and Nucleic Acids*; Wiley: New York, 1986.
13. Rance, M.; Sørensen, O. W.; Bodenhausen, G.; Wagner, G.; Ernst, R. R.; Wüthrich, K. *Biochem Biophys Res Commun* 1983, 117, 479–485.
14. Griesinger, C.; Otting, G.; Wüthrich, K.; Ernst, R. R. *J Am Chem Soc* 1988, 110, 7870–7872.
15. Anil-Kumar, Ernst, R. R.; Wüthrich, K. *Biochem Biophys Res Commun* 1980, 95, 1–6.
16. Bothner-By, A. A.; Stephens, R. L.; Lee, J.-M.; Warren, C. D.; Jeanloz, R. W. *J Am Chem Soc* 1984, 106, 811–814.
17. Marion, D.; Ikura, M.; Bax, A. *J Magn Reson* 1989, 84, 425–430.
18. DeMarco, A.; Wüthrich, K. *J Magn Reson* 1976, 24, 201–204.
19. Güntert, P.; Wüthrich, K. *J Magn Reson* 1992, 96, 403–407.
20. Güntert, P.; Dötsch, V.; Wider, G.; Wüthrich, K. *J Biomol NMR* 1992, 2, 619–629.
21. Bartels, C.; Xia, T.; Billeter, M.; Güntert, P.; Wüthrich, K. *J Biomol NMR* 1995, 5, 1–10.
22. Szyperski, T.; Güntert, P.; Otting, G.; Wüthrich, K. *J Magn Reson* 1992, 99, 552–560.
23. Griesinger, C.; Sørensen, O. W.; Ernst, R. R. *J Am Chem Soc* 1985, 107, 6394–6396.
24. Güntert, P.; Mumenthaler, C.; Wüthrich, K. *J Mol Biol* 1997, 273, 283–298.
25. Weiner, S. J.; Kollman, P. A.; Nguyen, D. T.; Case, D. A. *J Comput Chem* 1986, 7, 230–252.
26. Luginbühl, P.; Güntert, P.; Billeter, M.; Wüthrich, K. *J Biomol NMR* 1996, 8, 136–146.
27. Koradi, R.; Billeter, M.; Wüthrich, K. *J Mol Graph* 1996, 14, 51–55.
28. Riek, R. *NMR Structure of the Mouse Prion Protein*. ETH Dissertation No. 12759, 1998.
29. Bradley, E. K.; Thomason, J. F.; Cohen, F. E.; Kosen, P. A.; Kuntz, I. D. *J Mol Biol* 1990, 215, 607–622.
30. Lichtarge, O.; Jardetzky, O.; Li, Ch.-H. *Biochemistry* 1987, 26, 5916–5925.
31. Chaffotte, A.; Guillou, Y.; Delepiepierre, M.; Hinz, H.-J.; Goldberg, M. E. *Biochemistry* 1991, 30, 8067–8074.
32. Reymond, M. T.; Huo, S.; Duggan, B.; Wright, P. E.; Dyson, H. J. *Biochemistry* 1997, 36, 5234–5244.
33. Buck, M.; Radford, S. E.; Dobson, C. M. *Biochemistry* 1993, 32, 669–678.
34. Riek, R.; Wider, G.; Billeter, M.; Hornemann, S.; Glockshuber, R.; Wüthrich, K. *Proc Natl Acad Sci USA* 1998, 95, 11667–11672.
35. Presta, L. G.; Rose, G. D. *Science* 1988, 240, 1632–1641.
36. Richardson, J. S.; Richardson, D. C. *Science* 1988, 240, 1648–1652.
37. Dasgupta, S.; Bell, J. A. *Int J Pept Res* 1993, 41, 499–511.
38. Spera, S.; Bax, A. *J Am Chem Soc* 1991, 113, 5490–5492.